

# COMPOSITE SPATIAL MONTE CARLO INTEGRATION BASED ON GENERALIZED LEAST SQUARES

Kaiji Sekimoto<sup>1</sup> and Muneki Yasuda

Graduate School of Science and Engineering, Yamagata University, Japan

## Abstract

Although evaluation of the expectations on the Ising model is essential in various applications, this is frequently infeasible because of intractable multiple summations (or integrations). Spatial Monte Carlo integration (SMCI) is a sampling-based approximation, and can provide high-accuracy estimations for such intractable expectations. To evaluate the expectation of a function of variables in a specific region (called target region), SMCI considers a larger region containing the target region (called sum region). In SMCI, the multiple summation for the variables in the sum region is precisely executed, and that in the outer region is evaluated by the sampling approximation such as the standard Monte Carlo integration. It is guaranteed that the accuracy of the SMCI estimator is monotonically improved as the size of the sum region increases. However, a haphazard expansion of the sum region could cause a combinatorial explosion. Therefore, we hope to improve the accuracy without such region expansion. In this study, based on the theory of generalized least squares, a new effective method is proposed by combining multiple SMCI estimators. The validity of the proposed method is demonstrated theoretically and numerically. The results indicate that the proposed method can be effective in the inverse Ising problem (or Boltzmann machine learning).

## 1 Introduction

The Ising model, which is also known as Boltzmann machine in the machine-learning field [1, 2], is a traditional and important stochastic model in statistical mechanics. Some variants of Boltzmann machine, such as restricted Boltzmann machine (RBM) [3, 4] and deep Boltzmann machine (DBM) [5], exist. Boltzmann machines and its variants have developed mainly in the machine-learning field; however, recently, they are also actively investigated in physics [6, 7, 8, 9, 10]. The evaluation of expectations on the Ising model is quite fundamental in almost all applications of this model. However, this evaluation is infeasible in general because it contains multiple summations (or integrations) over all variables.

Monte Carlo integration (MCI) is one of the most popular methods for the evaluation of intractable expectations. In an Ising model with variables  $\mathbf{x} = \{x_i \mid i \in \mathcal{V}\}$  (where  $\mathcal{V}$  is the set of induces of all (discrete or continuous) variables), suppose that we want to obtain the expectation of function  $f_{\mathcal{T}}$  of variables in *target region*  $\mathcal{T} \subseteq \mathcal{V}$ . In MCI, the expectation is simply evaluated by the sample average of  $f_{\mathcal{T}}$  over a sample set that is generated from the Ising model using a sampling method, such as Gibbs sampling [11] and parallel tempering [12, 13]. Thus, an effective MCI, called *spatial Monte Carlo integration* (SMCI), was proposed [14, 15], which is a spatial extension of MCI. In SMCI, for the target region, region  $\mathcal{U}$ , which contains the target region as its subregion, is defined; particularly,  $\mathcal{U}$  is called *sum region* in SMCI. The expectation of function  $f_{\mathcal{T}}$  is evaluated as follows: multiple summation (or integration) over variables in the sum region is precisely executed, while multiple summation (or integration) over variables outside of the sum region is evaluated through sampling approximation similar to

---

<sup>1</sup>k.sekimoto1002@gmail.com

the standard MCI. SMCI has proven to be statistically more accurate than MCI, and its approximation accuracy is monotonically improved as the size of the sum region increases [14, 15]. Although an increase of the size of the sum region leads to an exponential increase of the computational cost, SMCI is practical when it is small. SMCI is effective in the inverse Ising problem [14, 16, 15, 17], which is also known as Boltzmann machine learning. Empirically, the SMCI-based learning method is better than some existing learning methods [16, 17], such as contrastive divergence [4], maximum pseudo-likelihood [18, 19], ratio matching [20], and minimum probability flow [21]. The detailed explanation of SMCI is described in section 3.

Suppose we have two different sum regions,  $\mathcal{U}_I$  and  $\mathcal{U}_{II}$ , for the purpose of the evaluation of  $f_{\mathcal{T}}$ . When  $\mathcal{U}_I \subset \mathcal{U}_{II}$ , we should select the SMCI estimator with  $\mathcal{U}_{II}$  because the estimator is guaranteed to be more accurate from the theory of SMCI. However, when an inclusion relation does not exist between both regions, which SMCI estimator is more accurate cannot be determined. A SMCI estimator with a larger sum region containing  $\mathcal{U}_I$  and  $\mathcal{U}_{II}$  is surely more accurate than the two SMCI estimators with  $\mathcal{U}_I$  and  $\mathcal{U}_{II}$ , respectively. However, a haphazard expansion of the sum region could cause a combinatorial explosion. We hope to obtain a more effective estimator without such a region expansion. In this paper, based on generalized least squares (GLS) [22, 23, 24], a method creating the desired estimator by combining the given SMCI estimators is proposed, referred to as *composite spatial Monte Carlo integration* (CSMCI). From the theory of GLS, an estimator obtained from CSMCI is guaranteed to be more accurate than its components (i.e., given SMCI estimators); furthermore, it is ensured to be the best unbiased estimator (BUE) (see section 4.1). However, unfortunately, CSMCI is not practical in general because it includes the evaluation of an intractable covariance matrix. We also propose an approximation of CSMCI for its implementation.

The remainder of this paper is organized as follows. The Ising model used in this study is defined in section 2. The detailed explanation of SMCI is provided in section 3. In section 4, we introduce the proposed method, that is, CSMCI, and subsequently, the validity of the estimators obtained from the proposed method is verified from both theoretical and experimental perspectives in sections 4.1 and 4.2, respectively. In section 5, we apply the proposed method to the inverse Ising problem, and then demonstrate its performance through numerical experiments. Finally, the summary and future works are described in section 6.

## 2 Ising Model

Consider an undirected graph,  $G(\mathcal{V}, \mathcal{E})$ , consisting of  $n$  vertices, where  $\mathcal{V} := \{1, 2, \dots, n\}$  is the set of vertices and  $\mathcal{E}$  is the set of undirected edges. The undirected edge between vertices  $i$  and  $j$  is labeled by  $(i, j)$  and labels  $(i, j)$  and  $(j, i)$  indicate the same edge. On the graph, an energy function (or a Hamiltonian) is defined as

$$E(\mathbf{x}; \theta) := - \sum_{i \in \mathcal{V}} h_i x_i - \sum_{(i, j) \in \mathcal{E}} J_{i, j} x_i x_j, \quad (1)$$

where  $\mathbf{x} := \{x_i \in \mathcal{X} \mid i \in \mathcal{V}\}$  is a set of random variables assigned on the vertices (here  $\mathcal{X}$  is the sample space of  $x_i$ ); and  $\{h_i\}$  and  $\{J_{i, j}\}$ , which are collectively denoted by  $\theta$ , are the external fields and exchange interactions, respectively. The exchange interactions are symmetric with respect to their induces, that is,  $J_{i, j} = J_{j, i}$ . Using the energy function in equation (1), an Ising model is expressed as

$$P_{\theta}(\mathbf{x}) := \frac{1}{Z(\theta)} \exp(-E(\mathbf{x}; \theta)), \quad (2)$$

where  $Z(\theta)$  denotes the partition function which is expressed as

$$Z(\theta) := \sum_{\mathbf{x}} \exp(-E(\mathbf{x}; \theta)), \quad (3)$$

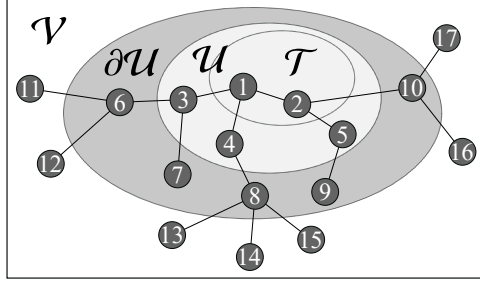


Figure 1: Illustration of the three regions for SMCI. In this illustration, the target, sum, and sample regions are  $\mathcal{T} = \{1, 2\}$ ,  $\mathcal{U} = \{1, 2, 3, 4, 5\}$ , and  $\partial\mathcal{U} = \{6, 7, 8, 9, 10\}$ , respectively.

where  $\sum_{\mathbf{x}} := \sum_{x_1 \in \mathcal{X}} \sum_{x_2 \in \mathcal{X}} \cdots \sum_{x_n \in \mathcal{X}} = \prod_{i \in \mathcal{V}} \sum_{x_i \in \mathcal{X}}$  is the summation over all possible realizations of  $\mathbf{x}$ ; when  $\mathcal{X}$  is a continuous space, the sum is replaced with the corresponding integration. The Ising model is known as a Boltzmann machine in the machine learning field [1]. The set of variables in a region  $\mathcal{A} \subseteq \mathcal{V}$  is denoted by  $\mathbf{x}_{\mathcal{A}}$  (i.e.,  $\mathbf{x}_{\mathcal{A}} = \{x_i \mid i \in \mathcal{A}\}$ ), and the summation over all possible realizations of  $\mathbf{x}_{\mathcal{A}}$  is denoted by  $\sum_{\mathbf{x}_{\mathcal{A}}} := \prod_{i \in \mathcal{A}} \sum_{x_i \in \mathcal{X}}$ .

On the Ising model, consider a function  $f$  of the variables in a *target region*  $\mathcal{T} \subseteq \mathcal{V}$ . The expectation of the function is written as

$$\mathbb{E}_{\theta}[f(\mathbf{x}_{\mathcal{T}})] := \sum_{\mathbf{x}} f(\mathbf{x}_{\mathcal{T}}) P_{\theta}(\mathbf{x}) = \sum_{\mathbf{x}_{\mathcal{T}}} f(\mathbf{x}_{\mathcal{T}}) P_{\theta}(\mathbf{x}_{\mathcal{T}}), \quad (4)$$

where  $P_{\theta}(\mathbf{x}_{\mathcal{T}}) = \sum_{\mathbf{x}_{\mathcal{V} \setminus \mathcal{T}}} P_{\theta}(\mathbf{x})$  is the marginal distribution of the Ising model. Except for some special cases, the evaluation of this expectation is computationally intractable because multiple summation whose cost exponentially grows with an increase with the size of the model. SMCI, described in the following section, is a sampling-based approximation that can effectively evaluate such an intractable expectation [14, 15].

### 3 Spatial Monte Carlo Integration

In this section, we briefly explain SMCI, based on the Ising model introduced in the previous section. Note that SMCI is applicable to general Markov random fields, including Ising models with many-body interactions.

Suppose that the set of i.i.d.  $N$  sample points,  $\mathcal{S} := \{\mathbf{s}^{(\mu)} \mid \mu = 1, 2, \dots, N\}$ , drawn from  $P_{\theta}(\mathbf{x})$  is obtained, where  $\mathbf{s}^{(\mu)} := \{s_i^{(\mu)} \in \mathcal{X} \mid i \in \mathcal{V}\}$  is the  $\mu$ th sample point. In the standard MCI, using the sample set  $\mathcal{S}$ , the true expectation in equation (4) is approximated by

$$\mathbb{E}_{\theta}[f(\mathbf{x}_{\mathcal{T}})] \approx \sum_{\mathbf{x}} f(\mathbf{x}_{\mathcal{T}}) Q_{\mathcal{S}}(\mathbf{x}) = \frac{1}{N} \sum_{\mu=1}^N f(\mathbf{s}_{\mathcal{T}}^{(\mu)}), \quad (5)$$

where  $\mathbf{s}_{\mathcal{T}}^{(\mu)}$  denotes the  $\mu$ th sample point on the target region  $\mathcal{T}$ ; that is,  $\mathbf{s}_{\mathcal{T}}^{(\mu)} := \{s_i^{(\mu)} \mid i \in \mathcal{T}\}$ . Here,  $Q_{\mathcal{S}}(\mathbf{x})$  is the empirical distribution (or the sample distribution) of  $\mathcal{S}$ , defined by

$$Q_{\mathcal{S}}(\mathbf{x}) := \frac{1}{N} \sum_{\mu=1}^N \prod_{i \in \mathcal{V}} \delta(x_i, s_i^{(\mu)}), \quad (6)$$

where  $\delta$  is the delta function (which is the Kronecker when  $\mathcal{X}$  is discrete or is the Dirac when  $\mathcal{X}$  is continuous).

In SMCI, for the target region, region  $\mathcal{U}$ , called the *sum region*, is introduced such that  $\mathcal{T} \subseteq \mathcal{U} \subseteq \mathcal{V}$ . Based on the sum region, the right-hand side of equation (4) can be decomposed as

$$\mathbb{E}_\theta[f(\mathbf{x}_\mathcal{T})] = \sum_{\mathbf{x}} f(\mathbf{x}_\mathcal{T}) P_\theta(\mathbf{x}_\mathcal{U} | \mathbf{x}_{\mathcal{V} \setminus \mathcal{U}}) P_\theta(\mathbf{x}_{\mathcal{V} \setminus \mathcal{U}}). \quad (7)$$

From the spatial Markov property of the Ising model, the conditional distribution in this equation is rewritten as

$$P_\theta(\mathbf{x}_\mathcal{U} | \mathbf{x}_{\mathcal{V} \setminus \mathcal{U}}) = P_\theta(\mathbf{x}_\mathcal{U} | \mathbf{x}_{\partial \mathcal{U}}), \quad (8)$$

where  $\partial \mathcal{U} := \{j | (i, j) \in \mathcal{E}, i \in \mathcal{U}, j \in \mathcal{V} \setminus \mathcal{U}\}$  denotes the outer adjacent region of  $\mathcal{U}$ , which is called the *sample region*. The illustration of the three regions (i.e., target, sum, and sample regions) for SMCI is shown in Figure 1. Using the conditional distribution in equation (8) and the marginalizing operation in equation (7) yields

$$\mathbb{E}_\theta[f(\mathbf{x}_\mathcal{T})] = \sum_{\mathbf{x}_\mathcal{U}} f(\mathbf{x}_\mathcal{T}) \sum_{\mathbf{x}_{\partial \mathcal{U}}} P_\theta(\mathbf{x}_\mathcal{U} | \mathbf{x}_{\partial \mathcal{U}}) P_\theta(\mathbf{x}_{\partial \mathcal{U}}). \quad (9)$$

The SMCI estimator for the true expectation is obtained by replacing  $P_\theta(\mathbf{x}_{\partial \mathcal{U}})$  in equation (9) with the corresponding marginal distribution of  $\mathcal{Q}_S(\mathbf{x})$ ; that is,  $\mathcal{Q}_S(\mathbf{x}_{\partial \mathcal{U}}) = N^{-1} \sum_{\mu=1}^N \prod_{i \in \partial \mathcal{U}} \delta(x_i, s_i^{(\mu)})$ :

$$m_\mathcal{T}(\mathcal{U}; \mathcal{S}) := \frac{1}{N} \sum_{\mu=1}^N \sum_{\mathbf{x}_\mathcal{U}} f(\mathbf{x}_\mathcal{T}) P_\theta(\mathbf{x}_\mathcal{U} | \mathbf{s}_{\partial \mathcal{U}}^{(\mu)}). \quad (10)$$

Equation (10) is the form of the sample average of the conditional expectation of  $f(\mathbf{x}_\mathcal{T})$ ,

$$f_{\mathcal{T}, \mathcal{U}}(\mathbf{s}_{\partial \mathcal{U}}^{(\mu)}) := \sum_{\mathbf{x}_\mathcal{U}} f(\mathbf{x}_\mathcal{T}) P_\theta(\mathbf{x}_\mathcal{U} | \mathbf{s}_{\partial \mathcal{U}}^{(\mu)}). \quad (11)$$

Such expression can be regarded as the so-called Rao-Blackwellization [25]. The simplest SMCI is the first-order SMCI (1-SMCI) method wherein the sum region is identical to the target region. For example, consider the 1-SMCI method to approximate the expectation  $f(x_i) = x_i$  in the case of  $\mathcal{X} = \{-1, +1\}$ . Because the target and sum regions are  $\mathcal{T} = \mathcal{U} = \{i\}$  and the sample region  $\partial \mathcal{U} = \partial i = \{j | (i, j) \in \mathcal{E}, j \in \mathcal{V} \setminus \{i\}\}$ , the conditional distribution is written as

$$P_\theta(\mathbf{x}_\mathcal{U} | \mathbf{s}_{\partial \mathcal{U}}^{(\mu)}) = P_\theta(x_i | \mathbf{s}_{\partial i}^{(\mu)}) = \frac{\exp[(h_i + \sum_{j \in \partial i} J_{i,j} s_j^{(\mu)}) x_i]}{2 \cosh(h_i + \sum_{j \in \partial i} J_{i,j} s_j^{(\mu)})}.$$

Therefore, equation (10) becomes

$$m_i(i, \mathcal{S}) = \frac{1}{N} \sum_{\mu=1}^N \sum_{x_i \in \{-1, +1\}} x_i P_\theta(x_i | \mathbf{s}_{\partial i}^{(\mu)}) = \frac{1}{N} \sum_{\mu=1}^N \tanh\left(h_i + \sum_{j \in \partial i} J_{i,j} s_j^{(\mu)}\right).$$

The estimator in equation (10) is unbiased because  $\mathbb{E}_S[m_\mathcal{T}(\mathcal{U}; \mathcal{S})] = \mathbb{E}_\theta[f(\mathbf{x}_\mathcal{T})]$ , where

$$\mathbb{E}_S[A] := \sum_{\mathbf{s}^{(1)}} P_\theta(\mathbf{s}^{(1)}) \sum_{\mathbf{s}^{(2)}} P_\theta(\mathbf{s}^{(2)}) \cdots \sum_{\mathbf{s}^{(N)}} P_\theta(\mathbf{s}^{(N)}) A \quad (12)$$

denotes the average over the sample set  $\mathcal{S}$ . Moreover, from this unbiasedness and the central limit theorem, the distribution of the SMCI estimator is found to asymptotically converge to a normal distribution whose mean is the true expectation for a sufficient large  $N$ . The following two asymptotic properties

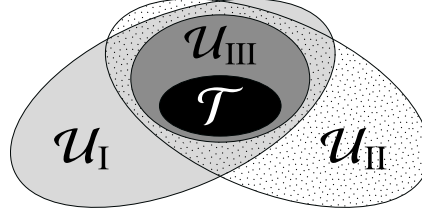


Figure 2: Illustration of the inclusion relation of the sum regions  $\mathcal{U}_I$ ,  $\mathcal{U}_{II}$ , and  $\mathcal{U}_{III}$ .

have been proved [14, 15]: for a given sample set, (i) SMCI is statistically more accurate than the standard MCI, and (ii) the accuracy of  $m_{\mathcal{T}}(\mathcal{U}_b; \mathcal{S})$  is statistically higher than that of  $m_{\mathcal{T}}(\mathcal{U}_a; \mathcal{S})$  when  $\mathcal{T} \subseteq \mathcal{U}_a \subseteq \mathcal{U}_b$ . From property (ii), the expansion of the sum region is theoretically guaranteed to statistically improve the approximation accuracy. However, in general, the expansion causes the exponential increase of the computational cost, except in some special cases (e.g., when the graph is a tree). When the cost of the evaluation of  $f(\mathbf{x}_{\mathcal{T}})$  is  $O(F)$  and  $\mathcal{X}$  is a discrete space, the cost of the evaluation of  $m_{\mathcal{T}}(\mathcal{U}; \mathcal{S})$  is estimated as  $O(NF|\mathcal{X}|^n)$ ; here, the cost of  $O(|\mathcal{X}|^n)$  is from the summation over  $\mathbf{x}_{\mathcal{U}}$ . Note that the cost of sampling does not consider in this cost evaluation.

Suppose that we have three different sum regions, namely,  $\mathcal{U}_I$ ,  $\mathcal{U}_{II}$ , and  $\mathcal{U}_{III}$ , for a fixed target region  $\mathcal{T}$ , and that their inclusion relation is as illustrated in Figure 2. From property (ii),  $m_{\mathcal{T}}(\mathcal{U}_I; \mathcal{S})$  and  $m_{\mathcal{T}}(\mathcal{U}_{II}; \mathcal{S})$  are statistically more accurate than  $m_{\mathcal{T}}(\mathcal{U}_{III}; \mathcal{S})$  because  $\mathcal{U}_{III} \subseteq \mathcal{U}_I$  and  $\mathcal{U}_{III} \subseteq \mathcal{U}_{II}$ . However, the accuracy of  $m_{\mathcal{T}}(\mathcal{U}_I; \mathcal{S})$  and  $m_{\mathcal{T}}(\mathcal{U}_{II}; \mathcal{S})$  is not theoretically compared because the relation of the two sum regions neither  $\mathcal{U}_I \subseteq \mathcal{U}_{II}$  nor  $\mathcal{U}_I \supseteq \mathcal{U}_{II}$ . In this case, it is difficult to select the best one. To address this problem, we consider an alternative approach in the subsequent section, in which a new estimator is created by combining multiple SMCI estimators obtained from different sum regions.

## 4 Composite Spatial Monte Carlo Integration

In this section, to ensure the approximation accuracy, we propose a new estimator based on the combination of multiple SMCI estimators obtained from different sum regions. Subsequently, we investigate the validity of the proposed method from theoretical and numerical perspectives in sections 4.1 and 4.2, respectively.

Suppose that we have  $K$  different sum regions that cover the target region  $\mathcal{T}$ ,  $\mathcal{U}_1, \mathcal{U}_2, \dots, \mathcal{U}_K \supseteq \mathcal{T}$ , to evaluate the true expectation in equation (4) based on SMCI. For the sample set  $\mathcal{S}$ , according to equation (10), we can obtain  $K$  different SMCI estimators for  $E_P[f(\mathbf{x}_{\mathcal{T}})]$  using the  $K$  different sum regions as

$$m_{\mathcal{T}}^{(k)} := m_{\mathcal{T}}(\mathcal{U}_k; \mathcal{S}) = \frac{1}{N} \sum_{\mu=1}^N f_{\mathcal{T}, \mathcal{U}_k}(\mathbf{s}_{\partial \mathcal{U}_k}^{(\mu)}), \quad k = 1, 2, \dots, K, \quad (13)$$

where  $f_{\mathcal{T}, \mathcal{U}_k}(\mathbf{s}_{\partial \mathcal{U}_k}^{(\mu)})$  is the conditional expectation for the  $k$ th sum region defined in equation (11). We collectively denote the  $K$  different SMCI estimators by the vector

$$\mathbf{m}_{\mathcal{T}} := (m_{\mathcal{T}}^{(1)}, m_{\mathcal{T}}^{(2)}, \dots, m_{\mathcal{T}}^{(K)})^t \in \mathbb{R}^K. \quad (14)$$

This vector can be regarded as the random vector whose elements (i.e.,  $K$  different SMCI estimators) are random variables. As mentioned in section 3, the SMCI estimators are unbiased, and their distributions asymptotically converge to normal distributions whose mean is the true expectation. However, the  $K$  different SMCI estimators are not statistical independent of each other because they share the same

sample set. From the multivariate central limit theorem, the distribution of  $\mathbf{m}_{\mathcal{T}}$  asymptotically converges to a multivariate normal distribution  $\mathcal{N}(\mathbf{m}_{\mathcal{T}} \mid \boldsymbol{\mu}, \boldsymbol{\Sigma})$  for a sufficient large  $N$ , whose mean vector is  $\boldsymbol{\mu} := \mathbb{E}_{\theta}[f(\mathbf{x}_{\mathcal{T}})]\mathbf{1}_K \in \mathbb{R}^K$  (here  $\mathbf{1}_K$  is the  $K$ -dimensional one vector) and whose covariance matrix  $\boldsymbol{\Sigma} \in \mathbb{R}^{K \times K}$  is defined as  $\Sigma_{k,k'} := \mathbb{E}_{\mathcal{S}}[m_{\mathcal{T}}^{(k)} m_{\mathcal{T}}^{(k')}] - \mathbb{E}_{\mathcal{S}}[m_{\mathcal{T}}^{(k)}] \mathbb{E}_{\mathcal{S}}[m_{\mathcal{T}}^{(k')}]$  (here  $\mathbb{E}_{\mathcal{S}}[\cdots]$  is the average over the sample set defined in equation (12)). Here,  $\boldsymbol{\Sigma}$  has been assumed to be positive definite. Since  $\mathbb{E}_{\mathcal{S}}[f_{\mathcal{T}, \mathbf{u}_k}(\mathbf{s}_{\partial \mathbf{u}_k}^{(\mu)})] = \mathbb{E}_{\theta}[f_{\mathcal{T}, \mathbf{u}_k}(\mathbf{x}_{\partial \mathbf{u}_k})] = \mathbb{E}_{\theta}[f(\mathbf{x}_{\mathcal{T}})]$  for all  $k$  and  $\mu$ ,

$$\Sigma_{k,k'} = \frac{1}{N} \mathbb{E}_{\theta} \left[ (f_{\mathcal{T}, \mathbf{u}_k}(\mathbf{x}_{\partial \mathbf{u}_k}) - \mathbb{E}_{\theta}[f_{\mathcal{T}, \mathbf{u}_k}(\mathbf{x}_{\partial \mathbf{u}_k})]) (f_{\mathcal{T}, \mathbf{u}_{k'}}(\mathbf{x}_{\partial \mathbf{u}_{k'}}) - \mathbb{E}_{\theta}[f_{\mathcal{T}, \mathbf{u}_{k'}}(\mathbf{x}_{\partial \mathbf{u}_{k'}})]) \right] \quad (15)$$

is obtained. Therefore, the relation,

$$\mathbf{m}_{\mathcal{T}} = \mathbb{E}_{\theta}[f(\mathbf{x}_{\mathcal{T}})]\mathbf{1}_K + \boldsymbol{\varepsilon}, \quad (16)$$

asymptotically holds for a sufficient large  $N$ , where  $\boldsymbol{\varepsilon} \in \mathbb{R}^K$  is the residual vector that is drawn from  $\mathcal{N}(\boldsymbol{\varepsilon} \mid \mathbf{0}_K, \boldsymbol{\Sigma})$ ; here,  $\mathbf{0}_K$  is the  $K$ -dimensional zero vector.

Regarding the relation of equation (16) as a linear regression problem, GLS provides the framework to create a new estimator for  $\mathbb{E}_{\theta}[f(\mathbf{x}_{\mathcal{T}})]$  using the given  $K$  SMCI estimators. In the context of GLS [22, 23, 24], we regard the “unknown” true expectation in equation (16) as regression coefficient  $\alpha$ ; that is,

$$\mathbf{m}_{\mathcal{T}} = \alpha \mathbf{1}_K + \boldsymbol{\varepsilon}. \quad (17)$$

Subsequently, as the elements of the residual vector are correlated, the optimal regression coefficient is obtained in terms of the minimization of the Mahalanobis distance; that is,

$$\hat{\alpha}_{\mathcal{T}} := \arg \min_{\alpha} (\mathbf{m}_{\mathcal{T}} - \alpha \mathbf{1}_K)^{\mathsf{t}} \boldsymbol{\Sigma}^{-1} (\mathbf{m}_{\mathcal{T}} - \alpha \mathbf{1}_K). \quad (18)$$

The resulting estimation  $\hat{\alpha}_{\mathcal{T}}$  is regarded as the approximation of the true expectation. The minimization of equation (18) yields

$$\hat{\alpha}_{\mathcal{T}} = \mathbf{c}^{\mathsf{t}} \mathbf{m}_{\mathcal{T}}, \quad (19)$$

where  $\mathbf{c} \in \mathbb{R}^K$  is the coefficient defined by

$$\mathbf{c} := \frac{1}{\Omega(\boldsymbol{\Sigma}^{-1})} \boldsymbol{\Sigma}^{-1} \mathbf{1}_K. \quad (20)$$

Here, for  $\mathbf{A} \in \mathbb{R}^{K \times K}$ ,  $\Omega(\mathbf{A}) := \mathbf{1}_K^{\mathsf{t}} \mathbf{A} \mathbf{1}_K \in \mathbb{R}$  denotes the sum of all elements of the assigned matrix.  $\hat{\alpha}_{\mathcal{T}}$  is the proposed estimator in this paper (hereinafter referred to as the CSMCI estimator). The CSMCI estimator is the linear combination of SMCI estimators. The CSMCI estimator is unbiased,  $\mathbb{E}_{\mathcal{S}}[\hat{\alpha}_{\mathcal{T}}] = \mathbb{E}_{\theta}[f(\mathbf{x}_{\mathcal{T}})]$ , and its variance is

$$\mathbb{V}_{\mathcal{S}}[\hat{\alpha}_{\mathcal{T}}] = \mathbf{c}^{\mathsf{t}} \boldsymbol{\Sigma} \mathbf{c} = \Omega(\boldsymbol{\Sigma}^{-1})^{-1} = O(N^{-1}), \quad (21)$$

where  $\mathbb{V}_{\mathcal{S}}[\mathbf{A}] := \mathbb{E}_{\mathcal{S}}[\mathbf{A}^2] - \mathbb{E}_{\mathcal{S}}[\mathbf{A}]^2$ . The CSMCI estimator given in equation (19) can be obtained from an alternative approach based on Lagrange multipliers; the detailed of explanation of which is described in the Appendix.

However, equation (15) includes intractable expectations, and the covariance matrix  $\boldsymbol{\Sigma}$  cannot be obtained; therefore, practically it has to be approximated (the so-called feasible GLS [23]). In this paper, it is simply approximated by the (unbiased) sample covariance matrix; that is,

$$\boldsymbol{\Sigma} \approx \boldsymbol{\Sigma}_{\text{app}} := \frac{1}{N} \left( \frac{1}{N-1} \sum_{\mu=1}^N \mathbf{r}_{\mu} \mathbf{r}_{\mu}^{\mathsf{t}} \right), \quad (22)$$

where  $\mathbf{r}_\mu \in \mathbb{R}^K$  is the vector whose  $k$ th element is defined as

$$r_{\mu,k} := f_{\mathcal{T},\mathcal{U}_k}(\mathbf{s}_{\partial\mathcal{U}_k}^{(\mu)}) - m_{\mathcal{T}}^{(k)}.$$

Therefore, the CSMCI estimator  $\hat{\alpha}_{\mathcal{T}}$  is approximated by

$$\hat{\alpha}_{\mathcal{T}} \approx \mathbf{c}_{\text{app}}^{\text{t}} \mathbf{m}_{\mathcal{T}}, \quad (23)$$

where

$$\mathbf{c}_{\text{app}} := \frac{1}{\Omega(\Sigma_{\text{app}}^{-1})} \Sigma_{\text{app}}^{-1} \mathbf{1}_K.$$

The estimator of equation (23) is referred to as quasi-CMSI (qCMSI) estimator. In practice, we use the qCMSI estimator instead of the CSMCI estimator of equation (19). Since  $\Sigma = \Sigma_{\text{app}} + O(1/\sqrt{N})$ , the qCMSI estimator converges to the CSMCI estimator as  $N$  increases. This implies that the qCMSI estimator converges to the true expectation in the limit of  $N \rightarrow \infty$ .

#### 4.1 Theoretical Validation

In this section, we discuss the validity of the CSMCI estimator in equation (19) without the covariance-matrix approximation in equation (22), from a theoretical perspective. From the result obtained in the Appendix, it is found that the CSMCI estimator  $\hat{\alpha}_{\mathcal{T}}$  is the best estimator, from the perspective of variance, among all unbiased estimators obtained by linear combinations of  $\mathbf{m}_{\mathcal{T}}$ ; thus, it is called best linear unbiased estimator (BLUE). The same result can be obtained from Gauss-Markov theorem in a rigorous manner [22, 23].

The fact of that the CMSI estimator is the BLUE immediately leads to the following two important properties. The first one is that the variance of the CMSI estimator is a lower bound of the variances of the  $K$  SMCI estimators,

$$V_S[\hat{\alpha}_{\mathcal{T}}] \leq \min_{k=1,2,\dots,K} V_S[m_{\mathcal{T}}^{(k)}], \quad (24)$$

because the CSMCI estimator is the BLUE and  $m_{\mathcal{T}}^{(k)}$  can be regarded as linear combination  $m_{\mathcal{T}}^{(k)} = \mathbf{v}^{\text{t}} \mathbf{m}_{\mathcal{T}}$ , the coefficients of which are  $v_k = 1$  and the others are zero. Equation (24) implies that the CMSI estimator is guaranteed to improve the approximation accuracy. The other one which described below can be led from the same fact. Consider  $(K+1)$  SMCI estimators obtained by adding a new SMCI estimator,  $m_{\mathcal{T}}^{(K+1)}$ , with a new sum region  $\mathcal{U}_{K+1} \supseteq \mathcal{T}$  to  $\mathbf{m}_{\mathcal{T}}$ :  $\mathbf{m}_{\mathcal{T}}^+ := (m_{\mathcal{T}}^{(1)}, m_{\mathcal{T}}^{(2)}, \dots, m_{\mathcal{T}}^{(K)}, m_{\mathcal{T}}^{(K+1)})^{\text{t}}$ . We denote the CSMCI estimator for the  $(K+1)$  SMCI estimators as  $\hat{\alpha}_{\mathcal{T}}^+$  obtained in a similar manner to equation (19). The following inequality holds:

$$V_S[\hat{\alpha}_{\mathcal{T}}^+] \leq V_S[\hat{\alpha}_{\mathcal{T}}]. \quad (25)$$

This inequality can be obtained from almost the same logic as that of equation (24) (i.e.,  $\hat{\alpha}_{\mathcal{T}}$  can be regarded as a linear combination of  $\mathbf{m}_{\mathcal{T}}^+$  in which the coefficient for  $m_{\mathcal{T}}^{(K+1)}$  is set to zero). Equation (25) implies that the accuracy of the CMSI estimator is monotonically improved by adding a new SMCI estimator.

Moreover, fortunately, from the theory of GLS, a stronger claim is possible in this case; that is, the CSMCI estimator is the BLUE (or minimum variance unbiased (MVU) estimator) [24]. This means that the CSMCI estimator is the best among all possible unbiased estimators obtained from  $\mathbf{m}_{\mathcal{T}}$  (not necessarily linear). This fact can be understood as follows. Since the distribution of the residual vector  $\varepsilon$

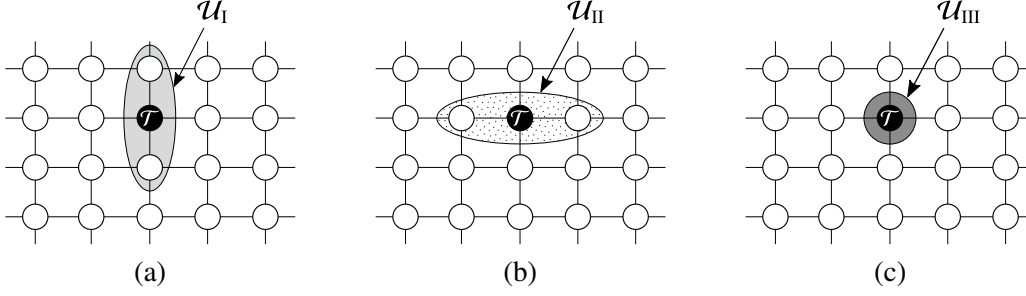


Figure 3: Three different sum regions, namely,  $\mathcal{U}_I$ ,  $\mathcal{U}_{II}$ , and  $\mathcal{U}_{III}$ , for  $\mathcal{T} = \{i\}$ .

is  $\mathcal{N}(\boldsymbol{\varepsilon} \mid \mathbf{0}_K, \boldsymbol{\Sigma})$ , the CSMCI estimator in equation (19) is the maximum likelihood (ML) estimator of the log-likelihood,

$$\ell(\alpha) := \ln \mathcal{N}(\mathbf{m}_{\mathcal{T}} \mid \alpha \mathbf{1}_K, \boldsymbol{\Sigma}) = -\frac{K}{2} \ln(2\pi) - \frac{1}{2} \ln \det \boldsymbol{\Sigma} - \frac{1}{2} (\mathbf{m}_{\mathcal{T}} - \alpha \mathbf{1}_K)^t \boldsymbol{\Sigma}^{-1} (\mathbf{m}_{\mathcal{T}} - \alpha \mathbf{1}_K), \quad (26)$$

with respect to  $\alpha$ , given  $\boldsymbol{\Sigma}$ . From the log-likelihood, the Fisher information is obtained as

$$\mathbb{E}_{\mathcal{S}} \left[ \left( \frac{\partial \ell(\alpha)}{\partial \alpha} \right)^2 \right]_{\alpha = \mathbb{E}_P[f(x_{\mathcal{T}})]} = \Omega(\boldsymbol{\Sigma}^{-1}).$$

From equation (21), evidently inverse of the Fisher information is equivalent to the variance of the CSMCI estimator, which implies that the variance of the CSMCI estimator achieves with the Cramér–Rao lower bound.

In this section, we discussed the validity of the proposed CSMCI estimator in equation (19) from the theoretical perspective. However, it is not a practical estimator because it needs to treat the intractable covariance matrix. Therefore, in practice, we have to use the CSMCI estimator together with a covariance-matrix approximation, e.g., the qCMSI estimator in equation (23). As mentioned in section 4, the qCSMCI estimator converges to the CSMCI estimator in the limit of  $N \rightarrow \infty$ . However, the above theoretical results are not guaranteed in the qCSMCI estimator in the case of a finite  $N$ . Thus, they are nothing more than *expectations* for the qCSMCI estimator in that case. Unfortunately, the unbiasedness of the qCSMCI estimator is not guaranteed. In the subsequent section, we demonstrate the validity of the qCMSI estimator through a numerical experiment.

## 4.2 Experimental Validation

In this section, we demonstrate the validity of the qCSMCI estimator in equation (23) through numerical experiments. For the experiments, we used the Ising model defined on a  $4 \times 5$  square grid graph with the periodic boundary condition (i.e., a torus graph) in which the sample space of the random variable was  $\mathcal{X} = \{-1, +1\}$  and  $h_i$  and  $J_{i,j}$  were independently drawn from an uniform distribution in the interval  $[-1/T, +1/T]$  (here  $T$  corresponds to the temperature). As the size of the present system is not large, the true expectation in equation (4) can be exactly computed.

On the Ising model, we considered to evaluate the uni-variable expectations; that is,  $\mathcal{T} = \{i\}$  and  $f(x_i) = x_i$ . For the target region, we considered three different sum regions:  $\mathcal{U}_I$ ,  $\mathcal{U}_{II}$ , and  $\mathcal{U}_{III}$ . Here,  $\mathcal{U}_{III}$  is the same as the target region, while  $\mathcal{U}_I$  and  $\mathcal{U}_{II}$  cover up to vertical and horizontal nearest-neighbor variables, respectively (see Figure 3). Since  $\mathcal{U}_I, \mathcal{U}_{II} \supseteq \mathcal{U}_{III} = \mathcal{T}$ , the SMCI estimators for  $\mathcal{U}_I$  and  $\mathcal{U}_{II}$  are guaranteed to be more accurate than that for  $\mathcal{U}_{III}$  from the theory of SMCI [14, 15]. The SMCI estimators with the three sum regions, namely,  $\mathcal{U}_I$ ,  $\mathcal{U}_{II}$ , and  $\mathcal{U}_{III}$ , are referred to as “SMCI-I,” “SMCI-II,” and “SMCI-III,” respectively. For the SMCI estimators, we considered two different



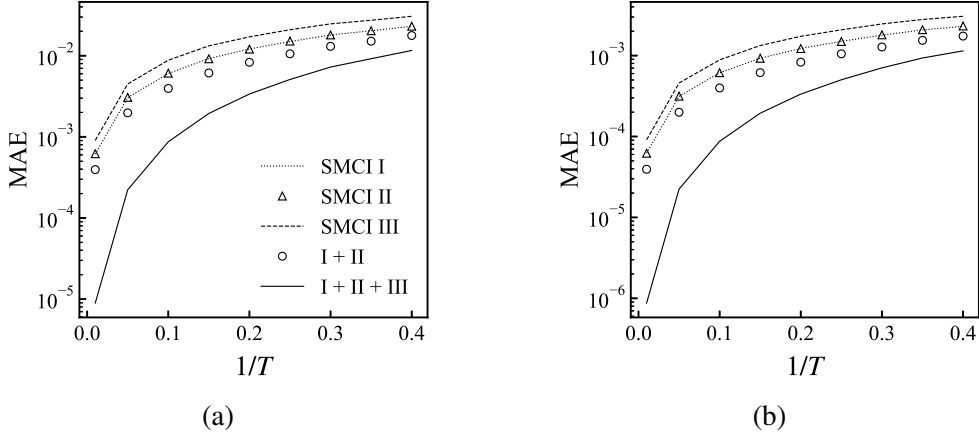


Figure 4: MAEs of the evaluation of  $E_\theta[x_i]$  for  $i \in \mathcal{V}$  versus  $1/T$  when (a)  $N = 100$  and (b)  $N = 10000$ . These plots are the average over 1000 experiments.

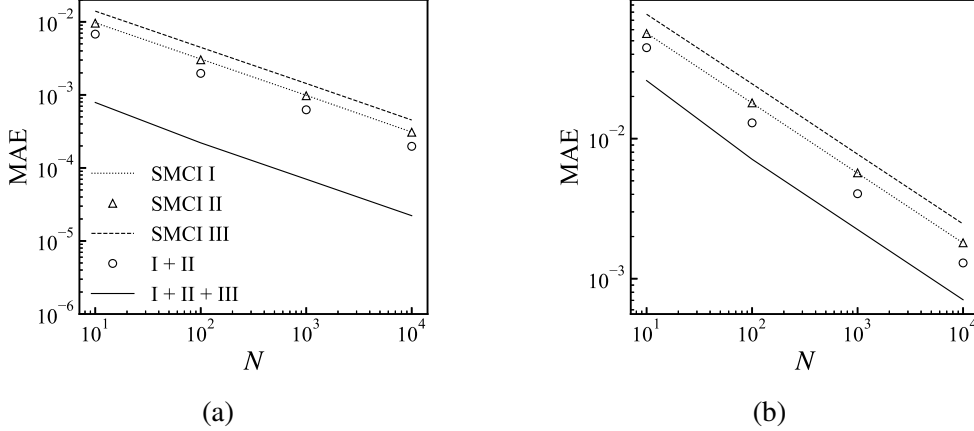


Figure 5: MAEs of the evaluation of  $E_\theta[x_i]$  for  $i \in \mathcal{V}$  versus  $N$  when (a)  $T = 0.05$  and (b)  $T = 0.3$ . These plots are the average over 1000 experiments.

qCSMCI estimators: the first one using SMCI-I and SMCI-II (referred to as “qCSMCI-I+II”) and the other one using all three SMCI estimators (referred to as “qCSMCI-all”). In the experiments, the sample set consisting of  $N$  sample points was obtained using Gibbs sampling. The approximation accuracy was measured by the mean absolute error (MAE) denoted by  $n^{-1} \sum_{i \in \mathcal{V}} |E_\theta[x_i] - E_{\text{app}}[x_i]|$ , where  $E_{\text{app}}[x_i]$  is a corresponding estimator obtained from the SMCI or qSMCI method.

Figure 4 shows the plots of the MAEs against  $1/T$ , where “I+II” and “I+II+III” denote the results obtained from the qCSMCI-I+II and qCSMCI-all, respectively. Evidently, the numerical results agree with the *expectations* from the theoretical results presented in section 4.1; that is, the CSMCI estimator improves the approximation accuracy and the accuracy of the CSMCI estimator is monotonically improved by adding a new SMCI estimator.

Figure 5 shows the plots of the MAEs against  $N$ . Clearly, the MAE of the qCSMCI estimators decrease at a speed approximately proportional to  $O(N^{-1/2})$ . As mentioned in section 4.1, the unbiasedness of the qCSMCI estimator is not theoretically guaranteed. However, its behavior appears quite similar to that of an unbiased estimator.

Finally, we discuss the computational efficiency of the qCSMCI estimator. From its definition, evidently that the computational cost of the qCSMCI estimator is higher than that of each SMCI component.

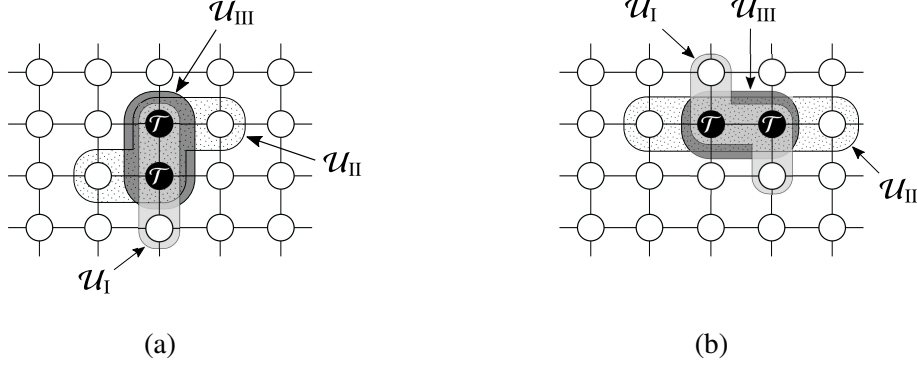


Figure 6: Three different sum regions, namely,  $\mathcal{U}_I$ ,  $\mathcal{U}_{II}$ , and  $\mathcal{U}_{III}$ , for  $\mathcal{T} = \{i, j\}$ : the cases of (a)  $i$  and  $j$  lining in a horizontal direction and (b)  $i$  and  $j$  lining in a vertical direction.

Suppose that the sum regions include at most a few variables. In this case, empirically, the sampling cost is dominant in the total procedure to evaluate an SMCI estimator (it occupies more than 99% in total in a case [26]) because the sampling procedure uses a costly pseudo-random-number generator. The difference of the evaluation costs of the qCSMCI estimator and its SMCI component can be small compared to the sampling cost. Meanwhile, in the results presented in Figure 5, the SMCI-I or SMCI-II needs about 10–1000 times larger  $N$  to achieve the same accuracy level of the qCSMCI-all. These facts support the computational efficiency of the qCSMCI estimator. However, a rigorous comparison of the costs is not straightforward because the costs complicatedly depend on several aspects, such as the structure of model, choice of sampling method, and setting of sum regions.

## 5 Application to the Inverse Ising Problem

In this section, we apply the proposed method to the inverse Ising problem, which is also known as the Boltzmann machine learning in the machine-learning field. Suppose that a set of  $N$  i.i.d. data points:  $\mathcal{D} := \{\mathbf{d}^{(\mu)} \mid \mu = 1, 2, \dots, N\}$ , where  $\mathbf{d}^{(\mu)} := \{d_i^{(\mu)} \in \mathcal{X} \mid i \in \mathcal{V}\}$  is the  $\mu$ th data point, is obtained. For dataset  $\mathcal{D}$ , consider that the log-likelihood is defined as

$$\psi(\theta) := \frac{1}{N} \sum_{\mu=1}^N \ln P_{\theta}(\mathbf{d}^{(\mu)}). \quad (27)$$

The inverse Ising problem aims for the maximization of this log-likelihood with respect to  $\theta$ , namely, the ML estimation based on the Ising model. The maximization is performed using a gradient ascent method. The gradients of the log-likelihood with respect to  $h_i$  and  $J_{i,j}$  are

$$\frac{\partial \psi(\theta)}{\partial h_i} = \frac{1}{N} \sum_{\mu=1}^N d_i^{(\mu)} - \mathbb{E}_{\theta}[x_i], \quad (28)$$

$$\frac{\partial \psi(\theta)}{\partial J_{i,j}} = \frac{1}{N} \sum_{\mu=1}^N d_i^{(\mu)} d_j^{(\mu)} - \mathbb{E}_{\theta}[x_i x_j]. \quad (29)$$

The first terms of these gradients are the sample averages of the dataset, and the second terms are the corresponding expectations of the Ising model. Because these gradients have the intractable expectations in their second terms, they have to be approximated to implement the ML estimation. We approximate these

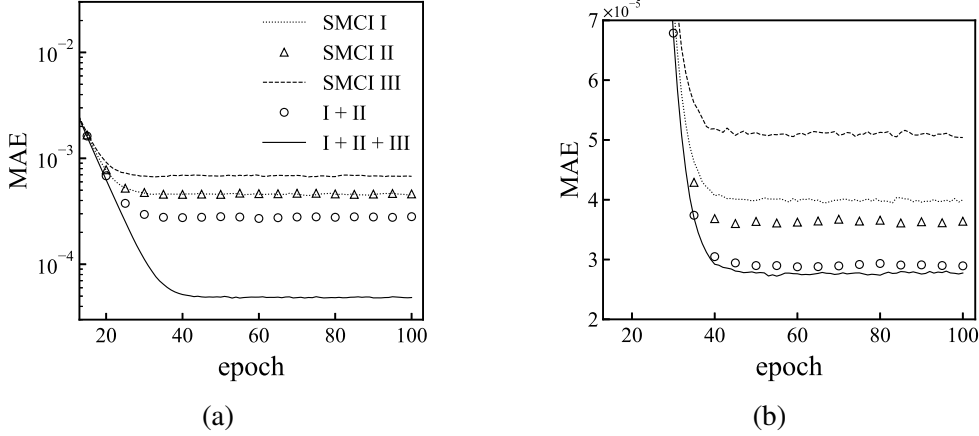


Figure 7: MAEs of (a)  $h_i$ s for  $i \in \mathcal{V}$  and (b)  $J_{i,j}$ s for  $(i, j) \in \mathcal{E}$  versus the learning epoch when  $1/T = 0.05$ . These results are the average over 500 experiments.

intractable expectations using the qCSMCI estimators proposed in section 4 and examine the effectivity of the approximation through numerical experiments.

In the experiments, two Ising models were used: the first one is regarded as the generative model that generates the dataset, and the other one is regarded as the learning Ising model that is used in the ML estimation. Both Ising models were defined on a torus graph with  $n = 20$  used in the experiments in section 4.2. The parameters  $h_i$  and  $J_{i,j}$  were independently drawn from an uniform distribution in the interval  $[-1/T, +1/T]$ , and the sample spaces of both models were  $\mathcal{X} = \{-1, +1\}$ . The dataset was obtained from the generative Ising model through Gibbs sampling. Because  $n$  is not large, we can obtain the exact ML estimations.

To approximate the intractable expectations in equations (28) and (29) based on the SMCI and qCSMCI estimators, the sample set obtained from the learning Ising model are required. To obtain the sample set efficiently, we used the learning procedure that is similar to persistent contrastive divergence [27], proposed in the literature [15]. The data extension rate [15] in the procedure was set to one. For the approximation of  $E_\theta[x_i]$ , the three different sum regions shown in Figure 3, which is the same setting in the experiments in section 4.2, were used; for  $E_\theta[x_i x_j]$ , three different sum regions shown in Figure 6 were used. In all experiments in this section, the learning rate (i.e., the step rate in the gradient ascent method) was set to 0.02.

In the experiments, the learning based on the SMCI estimators with the sum regions, namely,  $\mathcal{U}_I$ ,  $\mathcal{U}_{II}$ , and  $\mathcal{U}_{III}$ , are referred to as “SMCI-I,” “SMCI-II,” and “SMCI-III,” respectively. Here, note that the three sum regions were ones illustrated in Figure 3 for the estimators for  $E_\theta[x_i]$  in equation (28), while they were ones illustrated in Figure 6 for the estimators for  $E_\theta[x_i x_j]$  in equation (29). The SMCI-I corresponds to the 1-SMCI learning method, and the SMCI-II and SMCI-III corresponds to the semi-second-order learning method (without variable selection based on a greedy maximum independent set) proposed in the literature [15]. For the SMCI learning methods, we considered two different qCSMCI learning methods: the first one is using SMCI-I and SMCI-II (referred to as “qCSMCI-I+II”) and the other one is using all three SMCI estimators (referred to as “qCSMCI-all”). The accuracy of learning was measured by the MAEs of the parameters compared with the those obtained from the exact ML estimation. That is,  $n^{-1} \sum_{i \in \mathcal{V}} |h_i^{(t)} - h_i^{\text{ML}}|$  and  $|\mathcal{E}|^{-1} \sum_{(i,j) \in \mathcal{E}} |J_{i,j}^{(t)} - J_{i,j}^{\text{ML}}|$  were used, where  $h_i^{(t)}$  and  $J_{i,j}^{(t)}$  are the parameters obtained from the SMCI or qCSMCI method at  $t$ th update and  $h_i^{\text{ML}}$  and  $J_{i,j}^{\text{ML}}$  are the exact ML estimators. In all experiments, the initial values of the parameters were fixed to zero. Figures 7 and 8 show the MAEs against the learning epoch (i.e., the number of parameter updates), where  $N = 1000$ . In

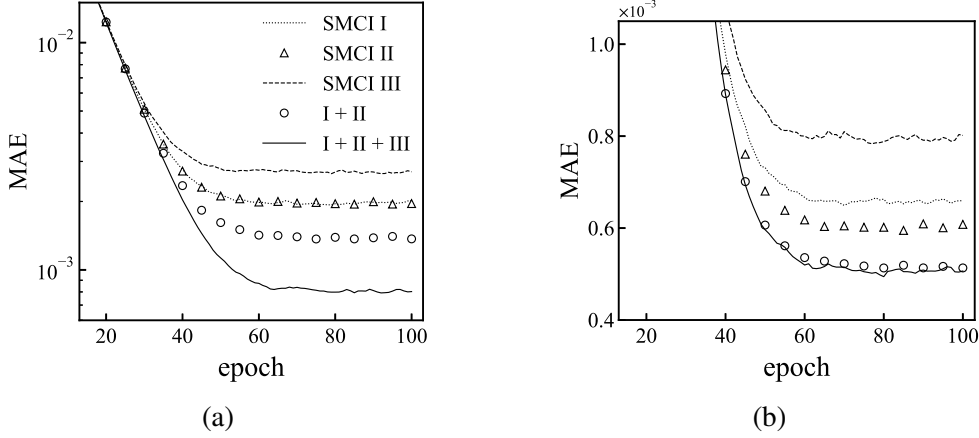


Figure 8: MAEs of (a)  $h_i$ s for  $i \in \mathcal{V}$  and (b)  $J_{i,j}$ s for  $(i, j) \in \mathcal{E}$  versus the learning epoch when  $1/T = 0.3$ . These results are the average over 500 experiments.

the figures, the results of “I+II” and “I+II+III” denote those obtained from qCSMCI-I+II and qCSMCI-all, respectively. We observe that the proposed qCSMCI method improves the learning accuracy.

## 6 Summary and Future Works

In this paper, we proposed a new estimator, called the CSMCI estimator, based on the theory of GLS, for an intractable expectation on the Ising model. The CSMCI estimator was obtained as a linear combination of multiple SMC I estimators,  $\mathbf{m}_{\mathcal{T}}$ , evaluating the same expectation (cf. equation (19)). The proposed CSMCI estimator (without the covariance-matrix approximation) has a good property; that is, the CSMCI estimator is the BLUE, as well as the BUE; this means that it is the best among all possible unbiased estimators obtained from  $\mathbf{m}_{\mathcal{T}}$  (not necessarily linear). This immediately leads to the following two properties: (1) the CSMCI estimator is guaranteed to improve the approximation accuracy and (2) the accuracy of the CSMCI estimator is monotonically improved by adding a new SMC I estimator (cf. section 4.1).

However, the CSMCI estimator has intractable covariance matrix  $\Sigma$ , which is the true covariance matrix among  $\mathbf{m}_{\mathcal{T}}$ . Therefore, for the purpose of the implementation, we proposed the qCSMCI estimator that is obtained by replacing  $\Sigma$  with the sample covariance matrix (cf. equation (23)). Unfortunately, these properties of the CSMCI estimator are not theoretically guaranteed in the qCSMCI estimator. However, as observed, the behavior of the qCSMCI estimator agrees with these properties of the CSMCI estimator in the numerical experiments in sections 4.2 and 5.

The most important problem of the proposed method is the approximation of  $\Sigma$ . As mentioned previously, we approximate it by the sample covariance matrix. However, a more appropriate approximation may exist. For example, an approach based on the ML estimation can be available. As discussed in section 4.1, the framework of GLS can be regarded as the ML estimation for the log-likelihood of equation (26). A simultaneous maximization of the log-likelihood with respect to  $\alpha$  and  $\Sigma$  will provide an alternative qCSMCI estimator. Finding a more effective approximation of  $\Sigma$  is addressed in our near-future research. Additionally, applications of the proposed method to more practical learning models (e.g., RBMs and DBMs) are an important problem, which will be addressed in our future project.

## Acknowledgment

This work was supported by JSPS KAKENHI (grant numbers: 18K11459, 18H03303, and 21K11778) and JEES / Softbank AI scholarship.

## Appendix: Approach Based on Lagrange Multipliers

The CSMCI estimator obtained in equation (19) can be obtained from an alternative strategy based on Lagrange multipliers. Consider an unbiased estimator  $\gamma_{\mathcal{T}}$  for  $E_{\theta}[f(\mathbf{x}_{\mathcal{T}})]$  expressed by a linear combination of the  $K$  SMCI estimators,  $\mathbf{m}_{\mathcal{T}}$ , as  $\gamma_{\mathcal{T}} := \mathbf{w}^{\top} \mathbf{m}_{\mathcal{T}}$ , where  $\mathbf{w} \in \mathbb{R}^K$  is the coefficient vector satisfying  $\sum_{k=1}^K w_i = \mathbf{w}^{\top} \mathbf{1}_K = 1$ . Through this constraint, the unbiasedness of this estimator is ensured:  $E_S[\gamma_{\mathcal{T}}] = E_{\theta}[f(\mathbf{x}_{\mathcal{T}})]$ . The variance of the estimator is

$$V_S[\gamma_{\mathcal{T}}] = \mathbf{w}^{\top} \Sigma \mathbf{w}, \quad (30)$$

where  $\Sigma$  is the covariance matrix of  $\mathbf{m}_{\mathcal{T}}$  discussed in section 4.

In the statistics perspective, the optimal  $\mathbf{w}$  minimizes the variance in equation (30). To find the optimal  $\mathbf{w}$ , we solve the optimization problem; that is,

$$\min_{\mathbf{w}} V_S[\gamma_{\mathcal{T}}] \quad \text{s.t.} \quad \mathbf{w}^{\top} \mathbf{1}_K = 1.$$

This optimization problem can be easily solved by using a Lagrange multiplier  $\lambda$ , i.e., we minimize the Lagrangian,

$$L(\mathbf{w}, \lambda) := V_S[\gamma_{\mathcal{T}}] - \lambda(\mathbf{w}^{\top} \mathbf{1}_K - 1),$$

with respect to  $\mathbf{w}$ . From the external conditions of the Lagrangian, the optimal  $\mathbf{w}$  is obtained as the form of

$$\mathbf{w} = \frac{1}{\Omega(\Sigma^{-1})} \Sigma^{-1} \mathbf{1}_K.$$

The optimal  $\mathbf{w}$  is equivalent to  $\mathbf{c}$  expressed in equation (20); therefore, the optimal  $\gamma_{\mathcal{T}}$ , in the perspective of the variance, is equivalent to the CSMCI estimator in equation (19).

## References

- [1] D. H. Ackley, G. E. Hinton, and T. J. Sejnowski: Cognitive science **9** (1985) 147.
- [2] Y. Roudi, E. Aurell, and J. Hertz: Frontiers in Computational Neuroscience **3** (2009) 1.
- [3] P. Smolensky: Parallel distributed processing: Explorations in the microstructure of cognition **1** (1986) 194.
- [4] G. E. Hinton: Neural computation **14** (2002) 1771.
- [5] R. Salakhutdinov and G. Hinton: Artificial intelligence and statistics, 2009, pp. 448–455.
- [6] A. Decelle and C. Furtlehner: Chinese Physics B **30** (2021) 040202.
- [7] J. Chen, S. Cheng, H. Xie, L. Wang, and T. Xiang: Physical Review B **97** (2018) 085104.

- [8] Y. Nomura and M. Imada: Physical Review X **11** (2021) 031034.
- [9] G. Torlai, G. Mazzola, J. Carrasquilla, M. Troyer, R. Melko, and G. Carleo: Nature Physics **14** (2018) 447.
- [10] G. Carleo and M. Troyer: Science **355** (2017) 602.
- [11] S. Geman and D. Geman: IEEE Transactions on Pattern Analysis and Machine Intelligence **6** (1984) 721.
- [12] R. H. Swendsen and J.-S. Wang: Physical Review Letters **57** (1986) 2607.
- [13] K. Hukushima and K. Nemoto: Journal of the Physical Society of Japan **65** (1996) 1604.
- [14] M. Yasuda: Journal of the Physical Society of Japan **84** (2015) 034001.
- [15] M. Yasuda and K. Uchizawa: Neural Computation **33** (2021) 1037.
- [16] M. Yasuda: Algorithms **11** (2018) 42.
- [17] T. Katsumata and M. Yasuda: Nonlinear Theory and Its Applications, IEICE **12** (2021) 377.
- [18] J. Besag: Journal of the Royal Statistical Society D (The Statistician) **24** (1975) 179.
- [19] E. Aurell and M. Ekeberg: Physical Review Letters **108** (2012) 090201.
- [20] A. Hyvärinen: Computational Statistics & Data Analysis **51** (2007) 2499.
- [21] J. Sohl-Dickstein, P. B. Battaglino, and M. R. DeWeese: Physical Review Letters **107** (2011) 220601.
- [22] A. C. Aitken: Proceedings of the Royal Society of Edinburgh **55** (1936) 42.
- [23] W. H. Greene: *Econometric analysis* (Pearson Education India, 2003).
- [24] Y. Lee, J. A. Nelder, and Y. Pawitan: *Generalized linear models with random effects: unified analysis via H-likelihood* (Chapman and Hall/CRC, 2018).
- [25] J. S. Liu: *Monte Carlo strategies in scientific computing* (Springer, 2001).
- [26] M. Yasuda and K. Sekimoto: Physical Review E **103** (2021) 052118.
- [27] T. Tieleman: Proceedings of the 25th international conference on Machine learning, 2008, pp. 1064–1071.